Biodegradation **13:** 117–130, 2002.

A detailed analysis of the mechanisms controlling the acceleration of 2,4-DCP monooxygenation in the two-tank suspended growth process

Elizabeth P. Dahlen[1,*] & Bruce E. Rittmann[2]
[1]*Exponent Failure Analysis Associates, 149 Commonwealth Drive, Menlo Park, CA 94025, USA;* [2]*Department of Civil Engineering, Northwestern University, 2145 Sheridan Road, Evanston, IL 60208-3109, USA (*author for correspondence: e-mail: edahlen@exponent.com)*

Accepted 1 May 2002

Key words: dichlorophenol, dissolved oxygen, monooxygenation, nicotinamide adenine dinucleotide, phenolics, regulation, specific growth rate, suspended growth

Abstract

The mechanisms underlying the observed acceleration of monooxygenation reactions in two-tank accelerator/aerator suspended growth system are evaluated in detail. The accelerator tank is characterized by a very high electron flow through reduced nicotinamide adenine dinucleotide (NADH + H^+), particularly when the retention-time ratio is small. Only a small fraction of the electron flow was diverted to oxygenation reactions, and the major sinks of NADH + H^+ were respiration and biomass synthesis. The main producer of NADH + H^+ is oxidation of acetate, a rapidly degraded electron-donor substrate. The half-maximum-rate concentration for oxygen used in respiration was 0.03 mg/L, while the half-maximum-rate concentration for oxygen used as a cosubstrate in monooxygenation was 0.18 mg/L. Thus, monooxygenations were more sensitive to oxygen limitation than was respiration. The NADH + H^+ concentration had a direct effect on the monooxygenation kinetics. The rate coefficients for both monooxygenation reactions were directly proportional to the specific growth rate in the accelerator, which supports that the accelerator tank caused an up-regulation of the monooxygenase content. Because the rate coefficients in the aerator tank were much larger than in the one-tank system, even though the specific growth rates were nearly the same, monooxygenases may have carried over from the accelerator tank to the aerator tank. Its higher concentration of 2,4-dichlorophenol (2,4-DCP) and the higher specific growth rate were the main reasons why the accelerator had faster kinetics for 2,4-DCP utilization than did the aerator tank. The apparently higher levels of monooxygenase in both tanks of the two-tank system also appears be a primary reason why its performance was substantially superior to that of the one-tank system in terms of 2,4-DCP removal.

Introduction

A companion paper (Rittmann & Dahlen, companion) showed that a novel two-tank configuration for suspended growth system significantly increased the removal kinetics for phenol and 2,4-dichlorophenol (2,4-DCP), substrates requiring initial monooxygenation reactions. The two-tank system involves an *accelerator tank*, which receives the influent and the return sludge, and an *aerator tank*, which receives the mixed liquor from the accelerator tank.

The conceptual basis (Rittmann & Dahlen, companion) for the accelerator tank is that its small volume, high concentration of electron-donor substrates, and controlled low concentration of dissolved oxygen (DO) make it a specialized zone that increases the kinetics for initial monooxygenation reactions. In particular, the accelerator conditions can enrich the biomass in: (1) reduced nicotinamide adenine dinucleotide (NADH + H^+), which is a cosubstrate for the monooxygenation reactions; and (2) the monooxygenase enzyme, which may be regulated by the specific growth rate. The accelerator tank also has higher donor-substrate concentrations, which also increase utilization kinetics.

The aerator tank that follows the accelerator tank is required to ensure good removal of biochemical oxygen demand (BOD), to allow biomass synthesis, and to control the overall system solids retention time (SRT). A settler, solids recycle, and solids wasting also are present and have their normal roles in suspended growth treatment process (Rittmann & McCarty 2001).

The experimental study by Rittmann & Dahlen (companion), which employed a bench-scale suspended growth system fed acetate, phenol, and 2,4-DCP, directly compared the performance of the two-tank system with the usual one-tank suspended growth system. The experimental results clearly demonstrated that the removal kinetics for phenol and 2,4-DCP were accelerated. For example, for the more slowly degraded 2,4-DCP:

- The average percentage removal was 93% in the two-tank system, compared to 74% in the one-tank system, even though the total system detention time was smaller for most of the two-tank experiments.
- The average volumetric and biomass-specific rates of removal were 50% and 100% greater, respectively, in the two-tank system.
- The greatest increase in the removal rates occurred when the retention-time ratio (i.e., the fraction of the total system volume in the accelerator tank) was 0.2 and the DO concentration in the accelerator was low, averaging between 0.2 and 0.54 mgO_2/L.
- The biomass in the accelerator tank was enriched in NADH + H^+ when the DO concentration was less than 0.25 mg/L.
- The accelerator tank had significantly increased specific growth rates, approaching 30 d^{-1} when the retention-time ratio was 0.06.

While the companion paper documents that the two-tank accelerator/aerator system accelerated detoxification reactions involving initial monooxygenase reactions, a more thorough evaluation is required to understand exactly how the two-tank system accomplished this goal. A detailed analysis is needed, because many mechanisms act, and sometimes they act in opposite directions. For example, a low DO concentration in the accelerator tank enriches the biomass in NADH + H^+, but it also can create serious oxygen limitation, since O_2 also is a cosubstrate for the monooxygenase reactions. Further, full-scale application of the two-tank approach will differ from the bench-scale experiments in important ways. For this reason, a mechanistic understanding is necessary to extrapolate the principles to practice.

The purpose of this paper is to provide a detailed, mechanistic view of the mechanisms acting in the two-tank process. In particular, we address these four issues: (1) how the accelerator tank affected electron flow among the various sources and sinks of NADH + H^+; (2) the competing effects of oxygen limitation and NADH + H^+ enrichment on monooxygenation kinetics; (3) the effect of the specific growth rate on the intracellular level of the monooxygenase enzyme; and (4) the relative effects of the different mechanisms.

Results and discussion

Electron flow among the various sources and sinks of NADH + H^+

Because the initial monooxygenation reactions require NADH + H^+ as a cosubstrate, they compete for available electrons with other electron-sinks: primarily respiration and biomass synthesis. In the experimental system, the main electron sources to create NADH + H^+ were oxidations of acetate, muconic acid, and chloromuconic acid (Rittmann & Dahlen, companion). The presence of the accelerator tank should alter the electron flow, since the accelerator tank has (Rittmann and Dahlen, companion):

- a high specific growth rate, which emphasizes the synthesis sink;
- a low DO concentration, which may restrict the respiration sink;
- increased degradation kinetics for phenol and 2,4-DCP, which are sinks and sources for NADH + H^+.

In order to compare the electron flows in each tank, we converted the measured rate of each reaction to equivalents of NADH + H^+ consumed or produced for each type of reaction. For example, the monooxygenation reactions for phenol and 2,4-DCP consume NADH + H^+ as a cosubstrate, but NADH + H^+ is produced by subsequent oxidation of ring-cleavage intermediates (Rittmann & Dahlen, companion). Figure 1 shows all the reactions and lists the stoichiometry for NADH + H^+ consumption or production. All soluble material that is not phenol, catechol, muconic acid, 2,4-DCP, 4-chlorocatechol, or chloromuconic acid is treated as acetate for the electron-flow computations. This material could include acetate, any intermediates from the partial oxidation of the muconic acids, and soluble microbial products (SMP)

(Namkung & Rittmann 1986; Rittmann & McCarty 2001). All materials included in the acetate category have the common feature of requiring no oxygenation reactions and, therefore, being only a net producer of NADH + H^+ when oxidized. All the phenols and catechols could be measured by high performance liquid chromatography (HPLC) (Rittmann & Dahlen, companion). No catechols were detected, which means that the phenols were taken at least to their muconic acids. For the electron-flow accounting, we assumed that the muconic acids were fully oxidized, because the biomass yields were consistent only with complete oxidation (Dahlen & Rittmann 2000).

We use the average values of the electron flows for the series of experiments performed at a retention-time ratio of 0.20 (series 1) to illustrate the consistent trends between the accelerator and aerator tanks. Table 1 shows the mass of each material consumed or produced per day normalized to the biomass and the conversion ratios between moles of NADH + H^+ and the moles of substrate. To give the O_2 respired, we subtracted the oxygen consumed in the mono- and di-oxygenation reactions and the oxygen demand of the biomass produced from the total oxygen demand of the substrate consumed.

The rates of NADH + H^+ equivalents consumed or produced, normalized to the biomass, are summarized in Table 2. The major producer of NADH + H^+ in the accelerator tank was the oxidation of acetate, which contributed 91% of the positive electron flow in the cells. This result underscores the importance of having a rapidly utilizable electron donor to supply electrons and drive all the electron-consuming reactions, including the monooxygenations. The largest electron sink was respiration (74%), but biomass synthesis accounted for 25%. This means that the cells invested only a small fraction of their total electron flow (1.1% here) into activation of the phenolic substrates by oxygenation reactions.

The main producers of NADH + H^+ in the aerator tank were the mineralization of muconic acids (59%) and acetate (27%). The primary consumer of NADH + H^+ was respiration (53%), although biomass synthesis also was a significant sink (39%). While the cells initially invested NADH + H^+ to break down the phenolic compounds, the net loss (8.1%) was relatively small compared to the NADH + H^+ invested to produce biomass or to the ultimate source of electrons from the activated substrates (the 73% from the muconic acids). Although the percentage of NADH + H^+ invested in monooxygenations was larger in the aerator tank, the absolute flow rate of electrons to monooxygenations was larger in the accelerator tank.

The trends in NADH + H^+ consumption and production for the middle retention-time ratio of 0.20 were generally reproduced by the average rates for each series of two-tank experiments. However, the magnitude of the rates in the accelerator tank increased as the retention-time ratio decreased, while rates were similar among all series for the aerator tank. Figures 2 and 3 summarize for each series of experiments as indicated by the experimental series retention time ratio the several flowrates of electrons in the accelerator and aerator tanks, respectively. Especially for the smallest retention-time ratios, the magnitudes of the rates for all reactions in the accelerator tank were substantially greater than the corresponding rates in the aerator tank. For example, the rate of NADH + H^+ consumption resulting from 2,4-DCP consumption at a retention-time ratio of 0.06 was 23 times higher in the accelerator tank than in the aerator tank. For a retention-time ratio of 0.32, it was 3 times greater. This means that the lower retention-time ratios created higher rates of electron flow through the cells in the accelerator, and the difference between the accelerator and aerator was greatest for the lowest retention-time ratio.

Competing effects of oxygen limitation and NADH + H^+ enrichment

The competing effects of oxygen limitation and NADH + H^+ enrichment can be represented quantitatively by Eqs 1 and 2:

$$r_1 = k_1 \frac{[\text{NADH}]}{[\text{X}]} \frac{[S_a]}{K'_a + [S_a]} \frac{[S_1]}{K_1 + [S_1]} [\text{X}] \quad (1)$$

$$r_2 = k_2 \frac{[\text{NADH}]}{[\text{X}]} \frac{[S_a]}{K'_a + [S_a]} \frac{[S_2]}{K_2 + [S_2]} [\text{X}] \quad (2)$$

in which subscript 1 refers to phenol, subscript 2 refers to 2,4-DCP, [NADH] is the μMol/L concentration of NADH + H^+, [X] is the mgVSS/L concentration of biomass, $[S_a]$ is the mg/L concentration of DO, $[S_1]$ is the mgCOD/L concentration of phenol, $[S_2]$ is the mgCOD/L concentration of 2,4-DCP, K'_a is the half-maximum rate concentration for DO used for monooxygenation (mgO_2/L), $K_{(1\,\text{or}\,2)}$ is the half-maximum-rate concentration for phenol or DCP monooxygenation (mgCOD/L), $k_{(1\,\text{or}\,2)}$ is a

Phenol overall stoichiometry

$$C_6H_6O + 14NAD^+ + 17H_2O \text{ === } 6H_2CO_3 + 14(NADH + H^+)$$

Monooxygenation of phenol

$$C_6H_6O + NADH + H^+ \text{ === } C_6H_6O_2 + H_2O + NAD^+$$

Dioxygenation of catechol

$$C_6H_6O_2 + O_2 \text{ === } C_6H_6O_4$$

Mineralization of *cis, cis* muconic acid

$$C_6H_6O_4 + 11NAD^+ + 14H_2O \text{ === } 6H_2CO_3 + 11(NADH + H^+)$$

Dichlorophenol overall stoichiometry

$$C_6H_4OCl_2 + 12NAD^+ + 17H_2O \text{ === } 6H_2CO_3 + 12(NADH + H^+) + 2HCl$$

Monooxygenation of dichlorophenol

$$C_6H_4Ocl_2 + 2(NADH + H^+) + O_2 \text{ === } C_6H_5O_2Cl + H_2O + 2NAD^+ + HCl$$

Dioxygenation of 4-chlorocatechol

$$C_6H_5O_2Cl + O_2 \text{ === } C_6H_5O_4Cl$$

Mineralization of chloromuconic acid

$$C_6H_5O_4Cl + 10NAD^+ + 14H_2O \text{ === } 6H_2CO_3 + 10(NADH + H^+) + HCl$$

Acetate mineralization

$$CH_3COOH + 4NAD^+ + 4H_2O \text{ === } 2H_2CO_3 + 4(NADH + H^+)$$

Biomass production

$$5H_2CO_3 + 10(NADH + H^+) + NH_3 \text{ === } C_5H_7O_2N + 10NAD^+ + 13H_2O$$

Respiration of oxygen

$$O_2 + 2(NADH + H^+) \text{ === } 2H_2O + 2NAD^+$$

Figure 1. Stoichiometry of the reactions that consume or produce NADH + H^+.

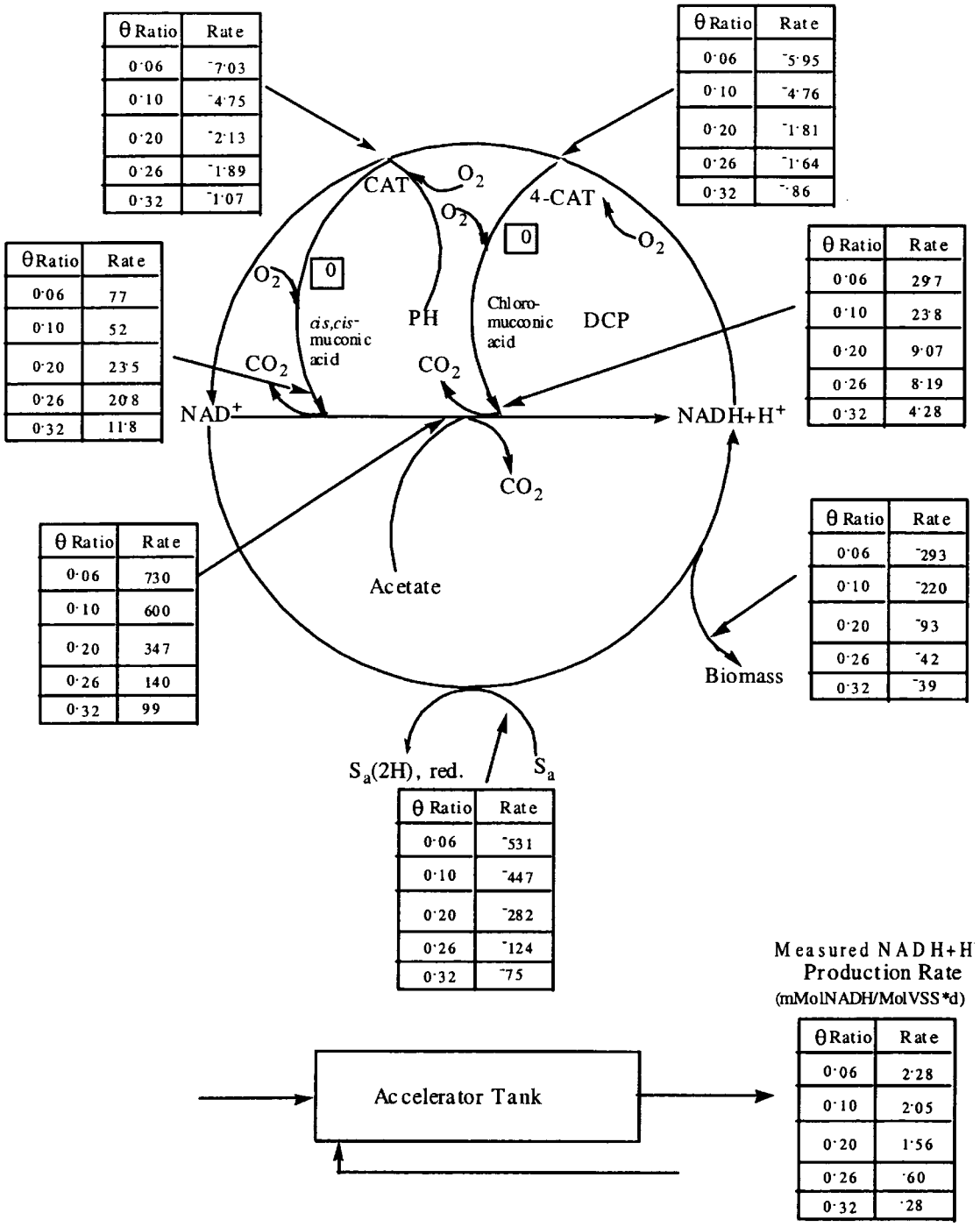

Figure 2. The rates of electron flow in the accelerator tank in MolNADH/MolVSS-d. Average data are presented for each series in the two-tank experiments.

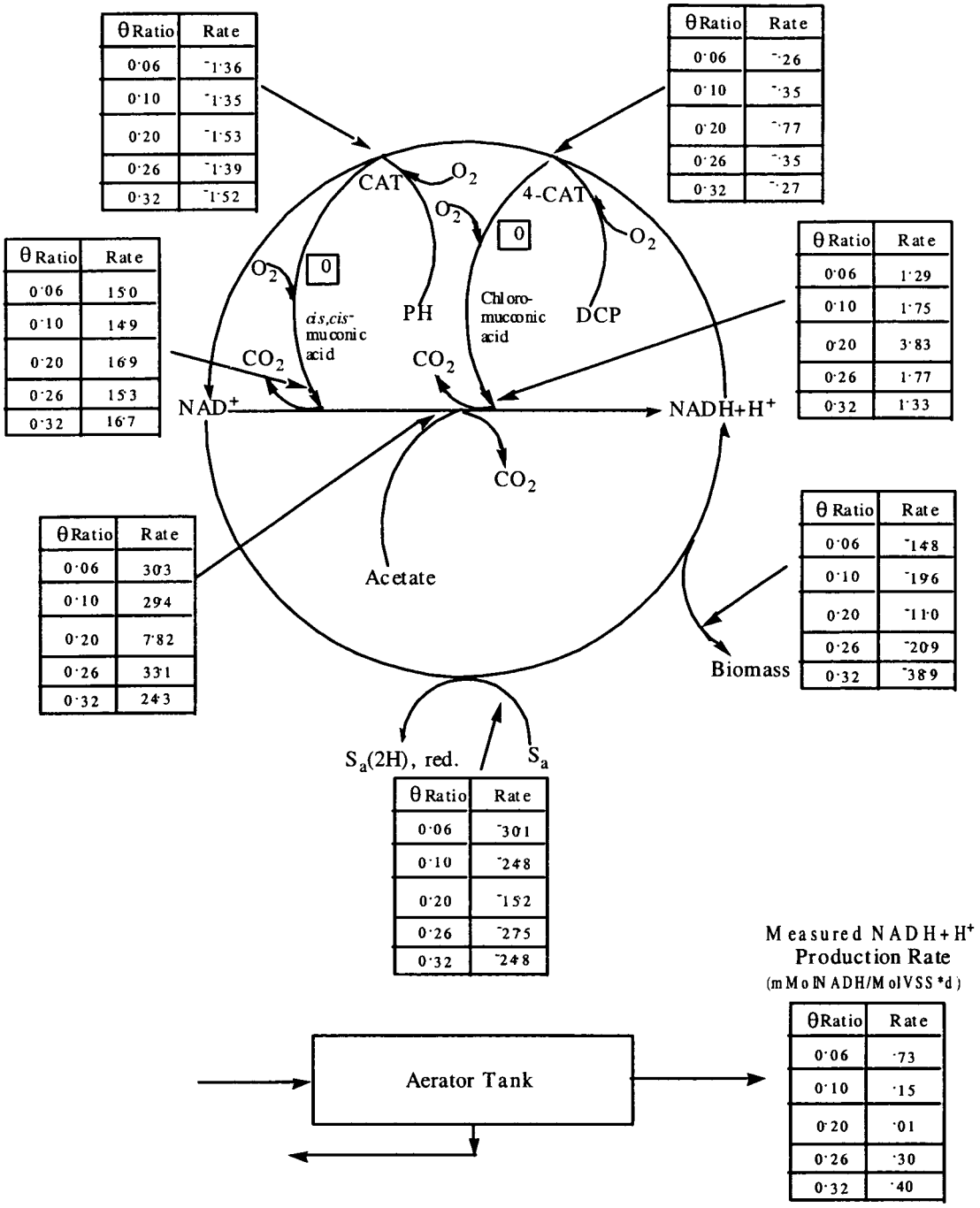

Figure 3. The rates of electron flow in the aerator tank in MolNADH/MolVSS-d. Average data are presented for each series of the two-tank experiments.

Table 1. The normalized mass rate of compound utilization in the two-tank reactor system and the conversion from substrate mass to NADH + H^+ for experimental series 4 (retention time ratio = 0.20)

Compound being degraded	Reactions consuming NADH + H^+?	Accelerator Rate of mass converted	Aerator rate of mass converted	Conversion ratios
Units		Molsubstrate/ MolVSS*day	Molsubstrate/ MolVSS*day	MolNADH + H^+/ Mol substrate
Dichlorophenol				
DCP → 4CAT	Yes, Monoox.	174	74	2MolNADH/MolDCP 1MolO_2/MolDCP
4CAT → Cyclo	Yes, Diox.	174	74	1MolO_2/Mol4CAT
Cyclo → CO_2	No	174	74	−10 MolNADH/MolCyclo
Phenol				
PH → CAT	Yes, Monoox.	477	343	1MolNADH/MolPH 1MolO2/MolPH
CAT → Muconic	Yes, Diox.	477	343	1MolO_2/MolCAT
Muconic → CO_2	No	477	343	−11MolNADH/MolPH
Acetate → CO_2	No	4,060	92	−4MolNADH/MolAc
Biomass production	Yes	1,490	177	−10MolNADH/MolBiomass
Respiration				
O_2 → energy	Yes	4,480	240	−2MolNADH/MolO_2

DCP = 2,4-dichlorophenol; 4CAT = r-chlorocatechol; cyclo = cycloisomerase; PH = phenol; CAT = catechol; and muconic = cis, cis miconic acid.

maximum-rate coefficient in mgCOD/μMolNADH-d, and $r_{(1\,\text{or}\,2)}$ is the biodegradation rate for phenol or 2,4-DCP in mgCOD/L-d. Furthermore, the rate of O_2 respiration can be represented by Eq. 3:

$$r_{\text{resp}} = k_{\text{resp}} \frac{[NADH]}{[\text{X}]} \frac{[S_a]}{K_a + [S_a]} [\text{X}] \qquad (3)$$

in which k_{resp} is the maximum-rate coefficient for respiration in mgO_2/μMolNADH-d, K_a is the half-maximum-rate concentration for DO used in respiration, and r_{resp} is the volumetric rate of respiration in MgO_2/L-d. The denominator of the specific NADH + H^+ content (i.e., [NADH]/[X]) cancels with [X] in Equations 1 to 3, simplifying the relationship to first-order in the concentration of NADH + H^+.

In this section, we evaluate the values of K_a' and K_a, and we also evaluate if the linear response in [NADH] was realized in the experiments. To evaluate the DO and NADH + H^+ effects, we analyzed the experimental data from series 4, in which the retention-time ratio was 0.06. Tables 3 through 5 summarize the experimental data from the six experiments comprising series 4. This set of data is valid for assessing the DO and NADH + H^+ effects, because the specific growth rate in the accelerator tank was nearly constant at 29 d^{-1}, but the specific content of NADH + H^+ varied substantially. As we show in the next section, the specific growth rate (μ) strongly affected the values of $k_{(1\,\text{or}\,2)}$, and it was necessary to have a stable μ in order assess the effects of DO and NADH + H^+. On the other hand, it was necessary to have a large variation in DO and NADH + H^+. Series 4 met all the criteria. The kinetic effects of DO and NADH + H^+ had to be evaluated together, because the content of NADH + H^+ was manipulated mostly by DO.

We first estimated the half-maximum-rate concentration for respiration, K_a, by performing a regression (Guttman et al. 1971; Sáez & Rittmann 1992, 1993) on the rate of acceptor utilization (r_{resp}) versus the acceptor product term on the right side of Equation 3: [NADH]{$[S_a]/(K_a + [S_a])$}. We simultaneously fit K_a and k_{resp} by varying the two parameters and computing the sum of squares of the absolute residuals (Sáez & Rittmann 1992; Guttman et al. 1971). We minimized the sum of squares of residuals, subject to having no systematic errors in the residuals and to having the regression line go through the origin. The best-fit K_a was 0.03 mgDO/L, and k_{resp} was 2.4×10^5 mgCOD/μMolNADH-d. Figure 4 shows the best fit, which had an r_2 value of 0.95. This K_a value is in the same range as those reported by Bae & Rittmann

Table 2. The rates at which the biomass produced or consumed NADH + H^+, normalized by the biomass concentration, for experimental series 1 (retention time ratio = 0.20)

Compound being degraded	Accelerator		Aerator	
	$NADH + H^+$ consumed	$NADH + H^+$ produced	$NADH + H^+$ consumed	$NADH + H^+$ produced
Units	MolNADH/ MolVSS-d (% of column total)	MolNADH/ MolVSS-d (% of column total)	MolNADH/ MolVSS-d (% of column total)	MolNADH/ MolVSS-d (% of column total)
Dichlorophenol				
DCP → 4CAT	1.81	.	0.77	
	(0.48%)	.	(2.70%)	
4CAT → Cyclo	.	0.0	.	0.0
	.	(0.00%)	.	(0.00%)
Cyclo → CO_2	.	9.07	.	3.83
	.	(2.39%)	.	(13.41%)
Phenol				
PH → CAT	2.13	.	1.53	
	(0.57%)	.	(5.41%)	
CAT → Muconic	.	0.0	.	0.0
	.	(0.00%)	.	(0.00%)
Muconic → CO_2	.	23.47	.	16.88
	.	(6.19%)	.	(59.16%)
Net acetate → CO_2	.	346.7	.	7.82
	.	(91.42%)	.	(27.42%)
Biomass production	92.8	.	11.04	
	(24.63%)	.	(38.93%)	
Respiration				
O_2 → energy	282.5	.	15.19	
	(74.33%)	.	(52.95%)	
Column total	379.2	379.2	28.53	28.53
Net production based on $NADH + H^+$ measurements (mMol $NADH + H^+$/Mol VSS*day)	1.56		0.01	

Table 3. Operating data for experimental series 4 (retention time ratio = 0.06)

Exp.	Q mL/min	Q_{rec} mL/min	Vol_{acc} mL	[DO] mgDO/L	COD_{in} (mgCOD/L)	$[PH]_{in}$ mgCOD/L	$[DCP]_{in}$ mgCOD/L
1	2.4	0.4	58	0.15	307	97	13.1
2	2.4	0.3	58	0.30	278	102	13.2
3	2.4	0.2	58	1.30	275	107	12.1
4	2.4	0.2	58	0.10	282	100	14.8
5	2.4	0.1	58	0.71	230	106	10.7
6	2.4	0.2	58	0.43	255	104	11.8

Table 4. Dissolved chemical concentrations for experimental series 4 accelerator tank

Exp.	COD_{acc} mgCOD/L	COD_{rec} mgCOD/L	$[PH]_{acc}$ mgCOD/L	$[PH]_{rec}$ mgCOD/L	$[DCP]_{acc}$ mgCOD/L	$[DCP]_{rec}$ mgCOD/L
1	247	64	81	0.74	8.72	0.30
2	210	78	86	0.30	8.70	0.72
3	224	100	94	0.88	8.39	0.62
4	178	84	85	0.48	8.48	0.40
5	174	99	96	0.34	7.08	0.44
6	188	133	86	0.59	6.40	0.23

Table 5. Biomass and $NADH + H^+$ concentrations and utilization rates for experimental series four accelerator tank

Exp	$[NADH + H^+]$ mMolNADH/L	[X] lmgVSS/L	$[X]_{rec}$ lmgVSS/L	Rate of acceptor	Rate of phenol Utilization, r_a	Rate of DCP Utilization, $r_{d,1}$ mgCOD/L*day	Utilization, r_2
1	7.4	15	75		1439	295	187
2	7.4	30	133		1611	309	205
3	4.9	45	400		1117	328	183
4	19.4	45	267		3483	516	335
5	5.8	40	523		1465	595	199
6	10.2	40	262		1896	623	292

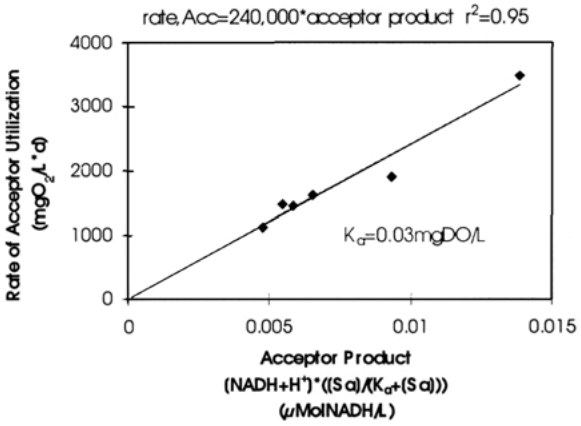

Figure 4. Rate of DO utilization versus the acceptor product (right-hand side of Equation 3) give the best-fit Ka = 0.03 mgO_2/L.

(1995) and Malmstead et al. (1995) for respiration of O_2.

We then used the rates of phenol and 2,4-DCP monooxygenation to estimate the half-maximum-rate concentration for DO when used as a cosubstrate (K'_a). We estimated a single K'_a value by performing regression of the rates of phenol *and* 2,4-DCP utilization versus their product terms from the right-hand sides of Eqs 1 and 2: $[NADH]\{[S_a]/(K'_a + [S_a])\}\{[S_{(1or2)}]/(K_{(1\,or\,2)} + [S_{(1\,or\,2)}])\}$. We already knew the K_1 and K_2 values from chemostat studies (Dahlen & Rittmann, 2000): K_1 = 0.8 mgCOD/L, and K_2 = 15.0 mgCOD/L. We assumed that K'_a was the same for phenol and 2,4-DCP utilization, since both substrates are likely utilized by the same monooxygenase (Dahlen & Rittmann, companion). We simultaneously fit K'_a, k_1, and k_2. The best fit was constrained to having the intercept go through the origin. We minimized the sum of squares of the absolute residuals for the utilization of *both* substrates.

The best-fit value of K'_a was 0.18 mgDO/L, and Figure 5 shows that the regression had no systematic errors to the residuals. The slopes gave the $k_{(1\,or\,2)}$ values:$k_1 = 7.8 \times 10^4$ mgCOD/μMolNADH-d, and $k_2 = 1.28 \times 10^5$ mgCOD/$a\mu$MolNADH-d. The r_2 values were 0.88 for phenol and 0.92 for 2,4-DCP. Consistent with K'_a values reported by Malmstead et al. (1995), this K'_a is significantly larger than K_a. It quantifies that oxygen limitation is likely to be much more significant for the monooxygenation reactions than for respiration.

Besides providing good estimates for K_a and K'_a, the analyses support that increasing the $NADH + H^+$

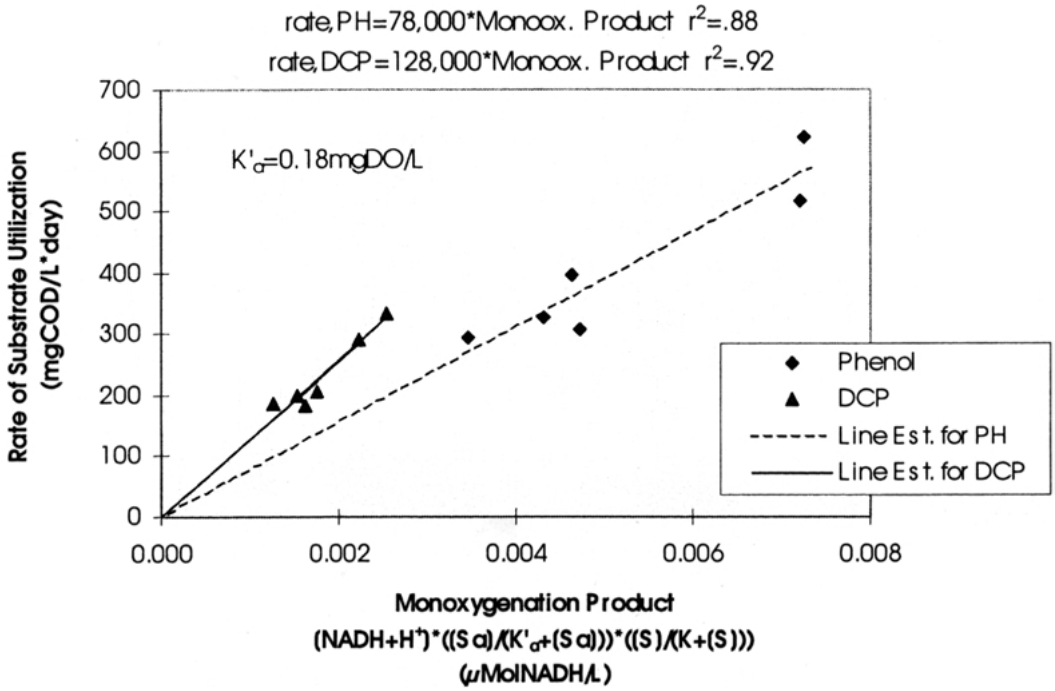

Figure 5. Rates of phenol and 2,4-DCP utilization (as mgCOD/L-d) versus the monooxygenation product (right-hand sides of Eqs 1 and 2) give the best-fit K'_a = 0.18 mgO_2/L.

content of the biomass accelerated the monooxygenation and respiration reactions in a manner similar to the first-order form shown in Eqs 1 to 3. Table 5 shows that the experiments had a nearly fivefold range of NADH + H^+ concentration, which means that NADH + H^+ had a large control over the product terms in Eqs 1 to 3. The good fits without systematic error in Figures 4 and 5 were possible only because the NADH + H^+ concentration had a strong, direct effect on the utilization rates.

Effect of specific growth rate on the intracellular level of the monooxygenase

The accelerator tank in the two-tank system was a zone in which the specific growth rate was very high compared to the aerator and to a one-tank system (Rittmann & Dahlen, companion). Based on past work (summarized in Rittmann & Dahlen, companion), we hypothesized that, as the specific growth rate increased in the accelerator, more monooxygenase enzyme was synthesized and available to catalyze all monooxygenase reactions. To evaluate this hypothesis, we performed regression of the product terms on the right-hand sides of Equations 1 and 2 for data from all the experimental series. Unlike series 4, which had a narrow range of μ values, the full set of experimental series had μ values from about 4 d^{-1} to almost 30 d^{-1} (Rittmann & Dahlen, companion). Using the K_a, K_1, and K_2 values from the previous section, we found the best-fit value of k_1 and k_2 for each series by minimizing the sum of squares of residuals, subject to no systematic errors. We did not constrain the regressions to go through the origin in this case. The plots of the phenol-utilization rates in the accelerator tank versus the product term on the right-hand side of Eq. 1 are presented in Figure 6. The slopes give the values of k_1 for each series. The analogous plots for 2,4-DCP are shown in Figure 7. For both substrates, the correlations show no systematic errors for each series of experiments, but each series has a unique value of $k_{(1\,or\,2)}$. Furthermore, the pattern of changing slope is the same for both substrates: an increasing $k_{(1\,or\,2)}$ with decreasing retention-time ratio.

The specific growth rate also varied inversely with the retention-time ratio (Rittmann & Dahlen, companion). Figure 8 plots the $k_{(1\,or\,2)}$ values from Figures 6 and 7 against the corresponding μ values from Rittmann & Dahlen (companion). The accelerator results have an almost perfect linear relationship between $k_{(1\,or\,2)}$ and μ. For each substrate, the slopes are positive, indicating that the maximum specific rate of

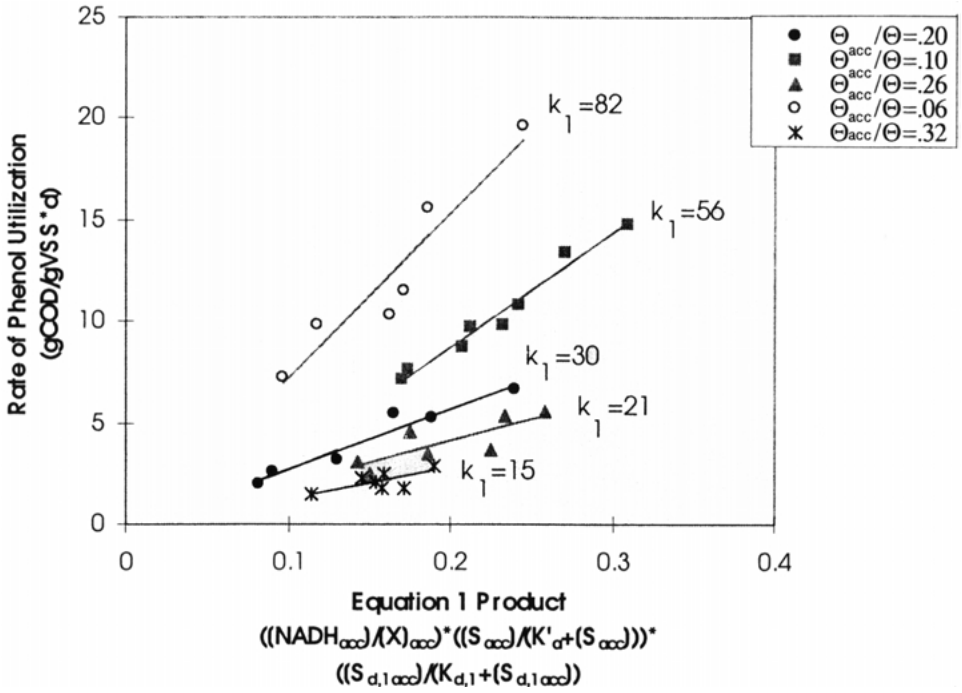

Figure 6. The rates of phenol utilization versus the right-hand side of Eq. 1 gives unique k_1 values for each series of experiments.

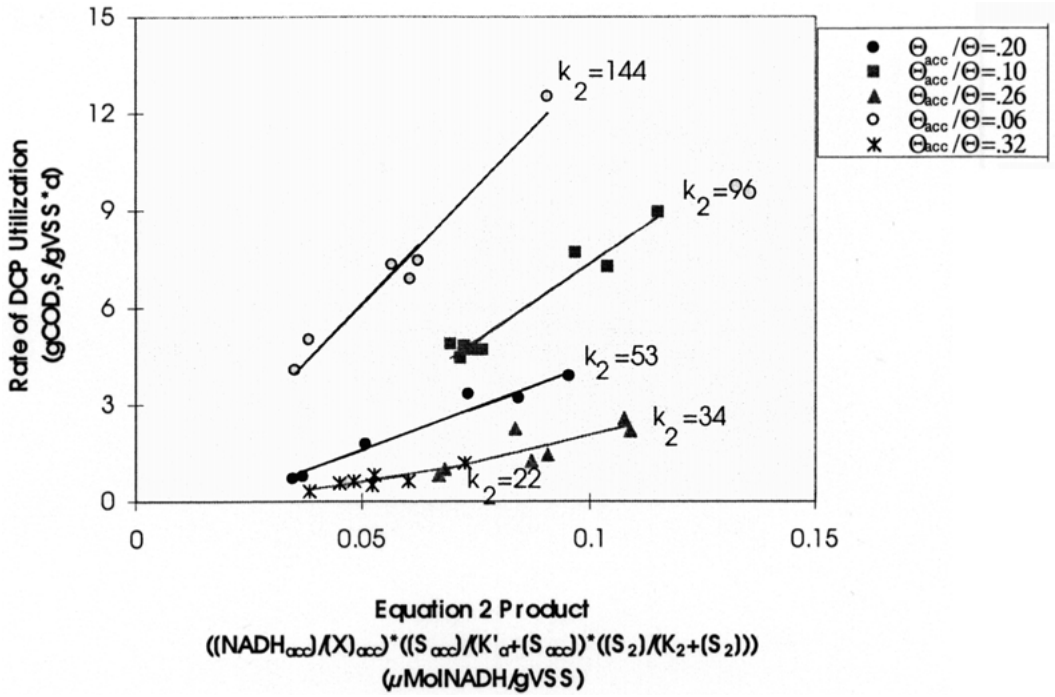

Figure 7. The rates of 2,4-DCP utilization versus the right-hand side of Eq. 2 give unique values of k_2 for each experimental series.

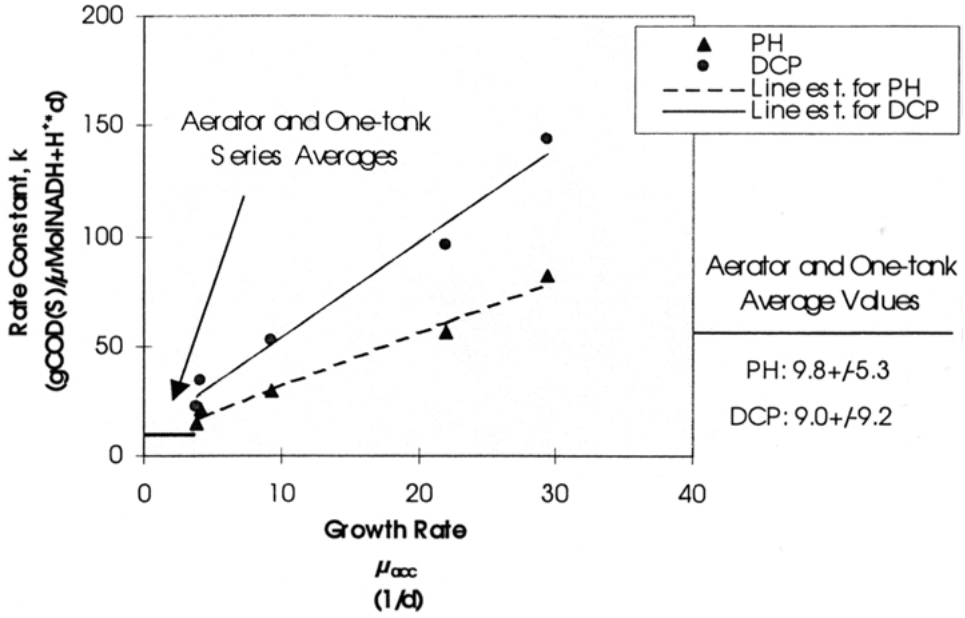

Figure 8. Phenol and 2,4-DCP rate coefficients ($k_{(1\,or\,2)}$, versus the specific growth rate (μ) show that $k_{(1\,or\,2)}$ was linearly proportional to μ for the accelerator conditions.

monooxygenation increases with the specific growth rate.

The maximum-rate coefficients should be proportional to the biomass' specific content of monooxygenase. Rittmann & Dahlen (companion) reviewed work by Balley et al. (1994), Baloo & Ramkrishna (1991), Xu et al. (1994), Fleming et al. (1993), and Yen & Serdar (1988), who saw that various catabolic enzymes were up-regulated when the specific growth rate was increased. As illustrated by Tsien et al. (1989) for oxidation of trichloroethene by methane monooxygenase, higher enzyme content translates into an increase in the specific utilization rate. The accelerator results shown in Figure 8 strongly support the hypothesis that the monooxygenase content was up-regulated by the high-μ conditions in the accelerator tank. The accelerator results in Figure 8 can be expressed mathematically by $k_{(1\,or\,2)} = \mu k'_{(1\,or\,2)}$, in which $k_{(1\,or\,2)}$ represents the maximum rate normalized to the enzyme content, expressed via μ. Based on Figure 8, k'_1 and k'_2 are 4,300 and 2,400 mgCOD/μMolNADH, respectively.

Also shown in Figure 8 are the average $k_{(1\,or\,2)}$ values for the aerator tank and the one-tank series of experiments. The μ and $k_{(1\,or\,2)}$ values for the aerator tank and one-tank series were relatively low, compared to the results from the accelerator tank. The specific growth rates for the aerator and one-tank series averaged 3.0 and 3.4 d^{-1}, respectively, and did not vary much (Rittmann & Dahlen, companion). The average k_1 and k_2 values were 9,800 and 9,000 mgCOD/mMolNADH-d for phenol and 2,4-DCP, respectively. Taken together, the $k_{(1\,or\,2)}$ values for the aerator and one-tank experiments are much lower than for the accelerator. However, the k_1 and k_2 values were not the same for the aerator tank and the one tank. The k_1 values were 2,800 and 10,700 mgCOD/μMolNADH-d, respectively, for the one-tank and aerator, while the k_2 values were 1,100 and 10,000 mgCOD/μMolNADH-day. Thus, the k_1 and k_2 values were substantially higher in the aerator than in the one-tank system. For instance, k_2 was 9 times larger in the aerator than in the one tank. This difference may be due to carry over of biomass that has been up regulated in the accelerator. Thus, the special conditions in the accelerator tank may be partially transferable to the aerator, thereby pointing out another potential advantage of the two-tank system.

Relative effects of the different mechanisms

When $\mu k_{(1\,or\,2)}$ is substituted for $k_{(1\,or\,2)}$ in Eqs 1 and 2, the kinetics for utilization of phenol and 2,4-DCP contain four variable terms: the specific growth rate (μ), representing the monooxygenase content; a first-order term for NADH + H^+; representing its role as a cosubstrate; and two hyperbolic terms representing

kinetic limitations by DO and the substrate undergoing monooxygenation. In this section, we analyze the relative effects of the four terms.

Table 6 summarizes the values of each term and the product of the terms for several characteristic results with 2,4-DCP. The first row is for the one-tank series, which provides a baseline for comparison. The second and third rows are the average values for all the accelerator and aerator tanks, and they give a good general view of how the two-tank system differs from the one-tank series and how the accelerator and the aerator differ from each other. The fourth and fifth rows are for the accelerator and aerator tanks for two-tank series 1 (retention-time ratio = 0.20), which had the fastest removal kinetics for 2,4-DCP. Rows 6 and 7 are for series 1 (retention-time ratio = 0.06), which had the highest accelerator specific growth rate. Row 8 repeats the one-tank pattern of row 1, except that the effect of the specific growth rate is divided by 9 to reflect the possible lack of carry over of monooxygenase enzyme in the one-tank system.

Table 6 shows that the greatest positive difference between the accelerator tank and the aerator tank occurred in the growth-rate and 2,4-DCP terms. The substrate term had the greatest positive effect on average, and its importance was amplified for the retention-time ratio of 0.20. The growth-rate effect became more dominant when the retention-time ratio was smaller, since the corresponding specific growth rate in the accelerator was very large. On average and when the retention-time ratio was small, the NADH + H^+ term showed a relative deceleration in the accelerator tank. The DO term always disfavored the kinetics in the accelerator. When all the terms are multiplied, the product shows that the accelerator tank gives faster kinetics than the aerator tank in all cases, although the greatest difference is for the retention-time ratio of 0.20, which was the series having the best overall removal of 2,4-DCP.

When the growth-rate effect in the one-tank system is essentially equivalent to that in the aerator (row 1 of Table 6), the product of all terms for the one tank is intermediate between the aerator and accelerator tanks. On the other hand, dividing the one-tank growth-rate term by 9 to reflect a lack of monooxygenase carry over (row 8) makes the product much smaller than for the aerator or the accelerator. Given that the one-tank system had substantially slower removal kinetics (and percentage removal) of 2,4-DCP than did any of the two-tank systems (Rittmann & Dahlen, companion), the row-8 scenario may be the more realistic basis for comparison. If so, the benefit of up-regulation of the monooxygenase in the accelerator is expanded by its carry over to the aerator, where the k_2 value is elevated over that possible in a one-tank system.

Conclusions

A detailed evaluation of the mechanisms underlying the acceleration of monooxygenation reactions in two-tank accelerator/aerator suspended growth system yields these main conclusions.

First, the accelerator tank is characterized by a very high electron flow through NADH + H^+, particularly when the retention-time ratio was small. Only a small fraction (about 1%) of the electron flow is diverted to oxygenation reactions, and the major sinks of NADH + H^+ were respiration (74%) and biomass synthesis (25%). The main producer of NADH + H^+ was oxidation of acetate (91%), which underscores the importance of having a supply of rapidly degraded electron-donor substrate.

Second, the half-maximum-rate concentration for oxygen used in respiration (K_a) was 0.03 mg/L, while the half-maximum-rate concentration for oxygen used as a cosubstrate in monooxygenation (K'_a) was 0.18 mg/L. Thus, monooxygenations were more sensitive to oxygen limitation than was respiration. The analyses to estimate K_a and K'_a also supported the direct effect of NADH + H^+ on the kinetics of monooxygenation.

The specific growth rate in the accelerator tank had a strong and linear effect on the rate coefficient for both monooxygenation reactions. This supports that the high specific growth rates in the accelerator tank caused an up-regulation of the monooxygenase content. An additional finding was that the rate coefficients in the aerator tank were much larger than in the one-tank system, even though the specific growth rates were nearly the same. This suggests that the up-regulated levels of monooxygenases carried over from the accelerator tank to the aerator tank.

Finally, the accelerator's higher concentration of 2,4-DCP and higher specific growth rate were the main reasons why it had faster kinetics for 2,4-DCP utilization than did the aerator tank. The growth-rate effect was accentuated for the smallest retention-time ratios. The apparently higher levels of monooxygenase in both tanks of the two-tank system may be a primary reason why its performance was substantially superior

Table 6. Comparison of the relative importance of the terms in the rate expressions for utilization of 2,4-DCP in the accelerator, aerator, and one tank

Terms in the rate equation	Experimental average values				
	Growth rate μ	Monod term for the carrier [NADH + H^+]	Term for oxygen $\frac{[S_a]}{K'_a+[S_a]}$	Term for 2,4-DCP $\frac{[S_2]}{K_2+[S_2]}$	Product
One-tank	3.4	1.06	0.98	0.22	0.77
Two-tank averages					
Accelerator	13.75	0.43	0.56	0.38	1.26
Aerator	3.01	1.53	0.98	0.05	0.23
Two-tank series 1, Retention-time ratio = 0.20					
Accelerator	9.0	0.90	0.64	0.41	2.1
Aerator	3.01	0.89	0.98	0.043	0.11
Two-tank series 4, Retention-time ratio = 0.06					
Accelerator	29.0	0.26	0.74	0.34	1.90
Aerator	3.01	1.50	0.98	0.045	0.20
	With growth-rate effect divided by 9 to account for no monooxygenase carry over				
One tank	0.38	1.06	0.98	0.22	0.086

to that of the one-tank system in terms of utilization kinetics and percentage removal of 2,4-DCP.

Acknowledgement

The authors acknowledge the financial support of the United States National Science Foundation through grant number BES9413824.

References

Bae W & Rittmann BE (1996) Responses of intracellular cofactors to single and dual limitations. Biotechnol. Bioeng. 49: 690–699

Bally M, Wilberg E, Kühni M & Egli T (1994) Growth and regulation of enzyme synthesis in the nitrilotriacetic acid (NTA)-degrading bacterium *Chelatobacter heintzii* ATCC 29600. Microbiology 140: 1927–1936

Baloo S & Ramkrishna D (1991) Metabolic regulation in bacterial continuous cultures: II. Biotech. Bioeng. 38: 1353–1363

Dahlen EP & Rittmann BE (2000) Analysis of oxygenation reactions in a multi-substrate system – a new approach for estimating substrate-specific true yields. Biotechnol. Bioengr. 70: 685–692

Fleming JT, Sanseverino S & Sayler GS (1993) Quantitative relationship between napthalene catabolic gene frequency and expression in predicting PAH degradation in soils at town gas manufacturing sites. Environ. Sci. Technol. 27: 1068–1074

Guttman I, Wilks SS & Hunter JS (1971) Introductory Engineering Statistics, 2nd ed. John Wiley & Sons, Inc., New York

Malmstead MJ, Brockman FJ, Valocchi AJ & Rittmann BE (1995) Modeling biofilm biodegradation requiring cosubstrates: the quinoline example. Water Sci. and Technol. 3191: 71–84

Namkung E & Rittmann BE (1986) Soluble microbial products (SMP) formation kinetics by biofilms. Water Research 20: 795–806

Rittmann BE & Dahlen EP. Companion paper. Two-tank suspended growth process for accelerating the detoxification kinetics of hydrocarbons requiring initial monooxygenation reactions, submitted

Rittmann BE & McCarty PL (2001) Environmental Biotechnology: Principles and Applications. McGraw-Hill Book Co., New York

Sáez PB & Rittmann BE (1992) Model-parameter estimation using least squares. Water Research 26: 789–796

Sáez PB & Rittmann BE (1993) Biodegradation kinetics of a mixture containing a primary substrate (phenol) and an inhibitory co-metabolite (4-chlorophenol). Biodegradation 4: 3–21

Tsien H-C, Brusseau GA, Hanson RS & Wackett LP (1989) Biodegradation of trichloroethylene by *Methylosinus trichosporium* OB3b. Appl. and Environ. Microbiol. 55(12): 3155–3161

Xu W-Z, Fukuhara J, Yamamoto K, Yomo T & Urabe I (1994) Random mutagenesis of glutamine synthetase from *Eschericia coli*: correlation between structure, activity, and fitness. J. of Fermentation and bioengineering 77(3), 252–258

Yen KM & Serdar, CM (1988) Genetics of naphthalene catabolism in *Pseudomonads*. CRC Crit. Rev. Microbiol. 15: 247–267